

LIFE EXPECTANCY STUDIES FOR LCLS-II PERMANENT MAGNET UNDULATORS*

M. Santana Leitner[†], D. Bruch, C.R. Field, D. Martinez-Galarce, R. McKee
H.-D. Nuhn, M. Rowen, S.W. Score, SLAC National Accelerator Laboratory, Menlo Park, USA

Abstract

LCLS-II at SLAC National Accelerator Laboratory will add a 4 GeV superconducting Linac to the existing 20 GeV copper structure. Electron beams from the two sources going through two new variable gap undulators will produce FEL from 200 keV to 5000 keV at up to 929 kHz, also reaching 20 keV at low frequency.

Such performance will be achieved by hybrid design undulators with NdFeB magnet blocks until radiation-induced demagnetization exceeds 0.01 %. This is a sizable challenge, as LCLS-II will carry 120 kW beams in both its soft (SXR) and hard (HXR) beam-lines. Even small fractional losses could be excessive if too frequent or not detected and aborted fast enough.

A model of SXR undulator was set for FLUKA [1, 2] radiation transport, including the segments, phase-shifters, quadrupoles, RFBPM, stands/pillars and interconnecting parts. Components were “installed” according to MAD files, which were also used to code the optics. Beam-loss/shower propagation was simulated for beam mis-steering, halo interactions and beam interception at wire scanners. Results help set limits on shut-off times, uniform loss levels and wire scanner use.

INTRODUCTION AND GOALS

The goal of this work is to establish guidelines that help control the demagnetization rates of LCLS-II SXR undulator permanent magnets. Three different situations will be studied, each defining an operational limit:

- Full beam mis-steered onto first undulator magnet → maximum MPS shut-off time
- Uniform constant beam loss along SXR beam-line → maximum allowable beam loss
- Beam finder wire scan → maximum number of beam scans

Allowable values are not meant to be sharp limits, as neither radiation generation mechanisms will be exactly like the ones simulated, nor radiation-induced demagnetization is fully understood. The latter aspect is briefly summarized below.

Permanent Magnet Damage Threshold

Permanent magnet demagnetization has been a subject of several irradiation experiments, with somehow scattered results. It is believed that this rather complex phenomena has at least two components, one linked to local heating

above the Curie temperature from dose imparted by radiation, and another one due to more profound changes to the material, such as nuclear reactions. Here we will focus on the first mechanism, purely related to dose, as for LCLS-II environment it should be more relevant.

Experiments carried out under similar radiation conditions and for identical magnet types suggest those could take up to 2500 Gy before demagnetization exceeds 0.01 %. On the other hand, conclusions from Schlarb [3] yield a lower limit, 700 Gy, yet within the same order of magnitude. Here comparisons will be made for the two limits, between which a gray zone will be defined where demagnetization risk would progressively grow.

Moreover, comparisons will be made at three levels:

Individual magnets: here we will look at the magnet with the highest dose and set limits accordingly.

Segments: a less pessimistic considers that the inductance deficiency of one magnet is, to same extent, balanced by the fields of less demagnetized neighboring magnets. This will lead to less stringent limits.

Entire undulator: the previous approach is extended to the entire undulator.

Simulation Set-Up

Simulations have been performed with FLUKA Monte Carlo Transport Code. Detailed geometrical models of the undulator segments, as well as other of components were build per CAD drawings, as shown in Fig. 1. Emphasis was made on features near the beam-line, and especially on the 173 permanent magnets of each undulator.

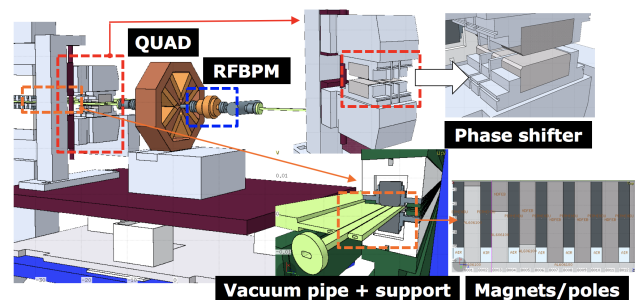


Figure 1: Flair [4] visualization of the models of LCLS-II SXR undulator, phase shifter, RFBPM, as implemented in FLUKA

These objects, together with generic implementations (based on basic parameters from the MAD8 files), were automatically replicated and placed along the beam-line with MadFLUKA beam-line builder [5]. Figure 2 shows the resulting geometry, which has 21 undulator segments,

* This work was supported by Department of Energy contract DE-AC02-76SF00515

[†] msantana@slac.stanford.edu

each with an upper and lower row of 173 permanent magnets (separated by poles). Between segments there are phase shifters, quadrupoles, RFBPMs, etc.

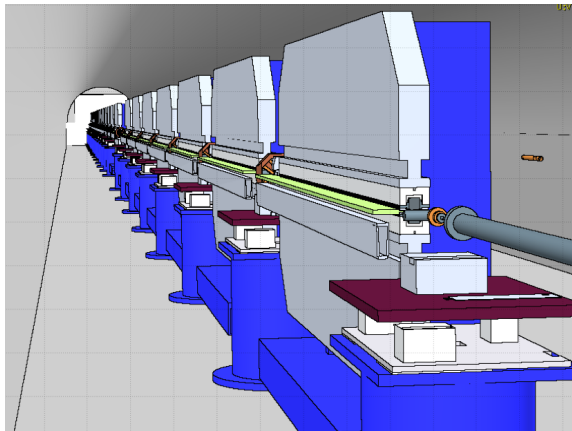


Figure 2: Rendering of the LCLS-II SXR undulator beamline as implemented for these studies

Verification of Optics

Beam optics plays an important role as it reshapes the electromagnetic showers along the undulator. Thus, verification of its appropriate implementation is key. For that purpose, particles were initiated with either a vertical or a horizontal displacement (of 30 μm), and transverse coordinates were registered at the passage through different components. The resulting curves are compared with the theoretical values in Fig. 3, showing excellent agreement in both transverse planes.

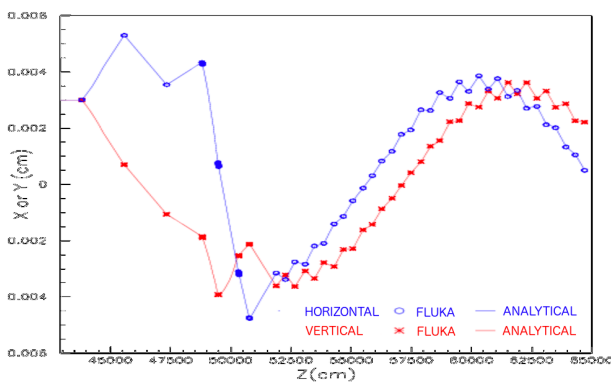


Figure 3: Simulated and theoretical transverse positions along SXR for 30 μm initial offset in either plane

RESULTS

MPS Shut-off Time for Beam Mis-Steering on Undulators

This study case reflects a hypothetical optics mis-match where the beam is fully mis-steered upwards at a glancing angle (1 mradian) onto the first undulator magnet. It is obvious

that such incident should be rapidly detected and terminated, but the question was what time scale would be required.

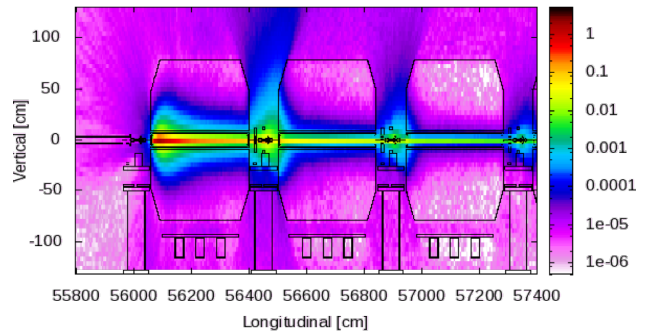


Figure 4: Elevation map at beam plane of the total fluence per mis-steered electron [cm²/e⁻] in the first three segments down-beam of the 1 mradian vertical mis-steering

Figure 4 shows how, due to the small impact angle, the radiation is nearly symmetrical over the horizontal plane. The radiation pattern in each segment is similar except for the intensity, which decreases slightly moving down-beam. It takes about 15 magnet/pole pairs to fully develop the shower within each sector. Then radiation is attenuated, and most of it is channeled through the segment aperture up to the break section, where it opens up to irradiate the following segment in a similar manner.

Table 1: Absorbed dose rate at the undulator magnets per Watt of mis-steered beam and associated required MPS shut-off time according to various criteria

Object	Dose rate [Gy/s/W]	t _r (700 Gy) [ms]	t _r (2500 Gy) [ms]
max(1 st)	1.20	17	5
<1 st >	0.16	130	36
< all >	0.008	2600	730

Table 1 summarizes the results of this test. The second column displays the maximum absorbed dose rate per each lost Watt [Gy/s/W] in a single magnet (row 2), as well as the maximum average value for an entire segment (row 3), and for all segments (row 4). The last two columns relate those numbers with the limits established earlier to define the maximum allowable time for machine protection systems to react, assuming a single such accident through the lifetime of the facility.

Maximum Allowable Uniform Normal Losses

The previous section addressed accidental beam losses. Here we investigate normal occurring beam losses (BL), representing interactions of beam halo or gas bremsstrahlung with the undulator chamber. Such events were modeled as axe-symmetrical, uniformly longitudinally distributed 1 mradian glancing losses.

As expected, resulting radiation fields are very similar for each undulator (Fig. 5), except for the first segment and the

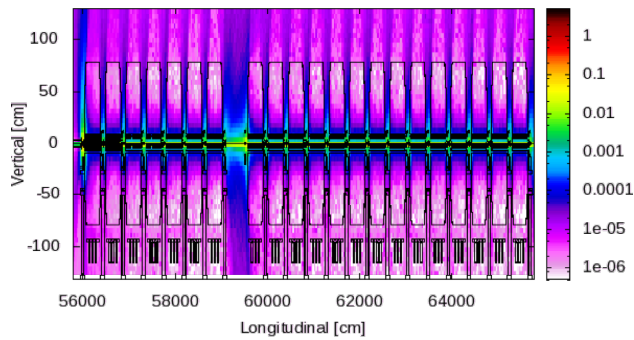


Figure 5: Elevation map at beam plane of the total fluence per lost electron along SXR beam-line [cm^2 / e^-]

segment just after the self-seeding chicane, as those are not in the immediate shade of up-beam components. Table 2 shows the absolute peak dose per Watt of beam uniformly lost, the peak average on a segment and the average on the SXR undulator, as well as the corresponding allowable loss level for 10-year survival at 5000 h/year operation.

Table 2: Absorbed dose rate at the undulator magnets per Watt of beam uniformly lost along SXR undulator, and allowed absolute amount such beam loss for different limiting criteria considering a 10-year life-time at 5000 hour operation

Object	Dose rate [Gy/s/W]	BL(700 Gy) [W]	BL(2500 Gy) [W]
max(1^{st})	0.07	0.05	0.2
< 1^{st} >	0.014	0.28	1.0
<all>	0.005	0.78	2.8

Dose from Beam Scans

A thin wire (WS34B) is planned to perform beam scans 79.3 m upstream of the first SXR undulator segment. In between the two, there will be several quadrupoles and a 116 cm-long, 30.48 cm side mask. In the current design, the wire has 30 μm diameter and it is made of graphite, while the aperture of the mask is 1.14 cm (horizontal) x 0.5 cm (vertical). Each beam scan will intercept 100 pulses, i.e. up to 2E11 electrons.

Dose absorbed by the permanent magnets will be mainly due to showers in those induced by Bremsstrahlung photons from the wire, with a small contribution from some deviated beam electrons. Figure 6 shows the estimated absorbed dose in the undulator magnets per beam scan, and Table 3 lists the corresponding numerical values and the maximum allowed number of scans.

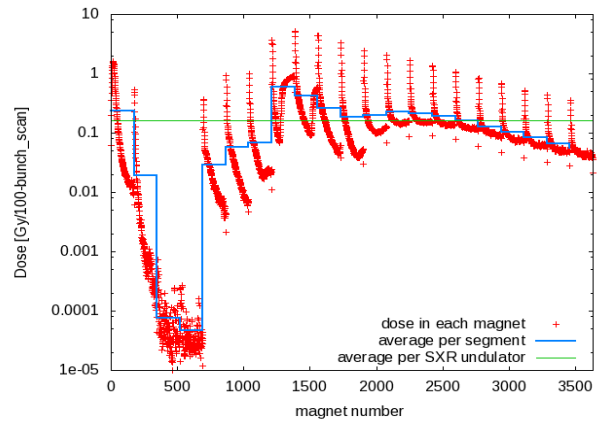


Figure 6: Absorbed dose in the individual magnets (red), in all magnets of each segment (blue), or in the entire set of SXR undulator magnets (green) per each 100 bunch beam scan ([Gy/scan])

Table 3: Dose on SXR magnets per each 100-pulse beam scan (SC) at WS34B, and allowable number of scans to reach 0.01 % demagnetization

Object	Dose rate [Gy/scan]	SC(700 Gy)	SC(2500 Gy)
max(1^{st})	3.00	233	833
< 1^{st} >	0.60	1116	4100
<all>	0.16	4375	15625

CONCLUSION

Estimated dose imparted to LCLS-II undulator magnets for various beam loss scenarios anticipate requirements in terms of MPS reaction time (millisecond scale), uniform sustained dose level (sub-watt), and a quota for beam finder scans (several thousand) that seem achievable for LCLS-II.

REFERENCES

- [1] T. T. Böhlen, F. Cerutti, M. P. W. Chin, A. Fassò, A. Ferrari, P. G. Ortega, A. Mairani, P. R. Sala, G. Smirnov and V. Vlachoudis, "The FLUKA Code: developments and challenges for high energy and medical applications", Nucl. Data Sheets, vol. 120, pp. 211-214, 2014
- [2] A. Ferrari, P. R. Sala, A. Fassò, and J. Ranft, "FLUKA: a multi-particle transport code", CERN, Geneva, Switzerland, Rep. CERN-2005-10, 2005, INFN/TC_05/11, SLAC-R-773
- [3] H. Schlarb, "Collimation System for the VUV Free-Electron Laser at the TESLA Test Facility/Title of thesis", Ph.D. thesis, Universität Hamburg, Germany, 2001.
- [4] V. Vlachoudis, "FLAIR: A powerful but user friendly graphical interface for FLUKA", in Proc. Int. Conf. on Mathematics, Computational Methods & Reactor Physics (M&C 2009), Saratoga Springs, New York, 2009.
- [5] M. Santana-Leitner et al., "MadFLUKA Beam Line 3D Builder. Simulation of Beam Loss Propagation in Accelerators", IPAC14 proceedings, MOPME040